Production of menthol-loaded nanoparticles by solvent displacement

Ferri A.[*], Kumari N., Peila R. and Barresi A. A.

Department of Applied Science and Technology, Politecnico di Torino
Corso Duca degli Abruzzi 24, 10129 Torino (Italy)

Supplementary material

to the article published in

Canadian Journal Chemical Engineering

(special issue GRICU 2016)

filed with: Depository for Unpublished Data, CISTI,
National Research Council Canada, Ottawa, Ontario, Canada K1A 0S2

[*] Corresponding author.

Chemicals

The main physical properties of menthol are reported in Table S1.

Table A1 Chemico-physical properties of racemate menthol.

Molecular weight (g/mol)	156.27
Melting temperature (°C)	30-32
Density (kg/m^3)	895
LogK_{ow}	3.4
$\Delta H_{melting}$ (kJ/mol)	10.25–12.83
Vapour pressure (hPa)	0.085 at 25°C

Influence of solvent type on nanoparticle size

The results confirm that the particle size decreased with increasing feed velocity and increased with increasing polymer concentration: the trend can be described by a power-law equation, at least in the turbulent range for Re_j>310. The trend is similar for acetone, acetonitrile and THF, but particles are significantly larger than in acetone at the same operating conditions (see a direct comparison in Figure S1).

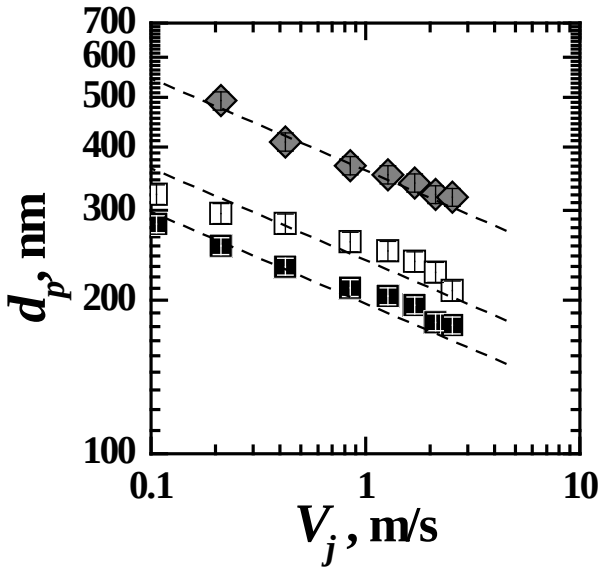

Figure S1. Influence of different solvents and inlet feed velocity on unloaded PCL particles size: ■, acetone; □, acetonitrile; ◆, THF. Inlet polymer concentration, C_{PCL}: 3 mg/mL; *QR*=0.5. CIJM mixer. Trend line have been calculated using Eq. (3) with β= – 0.18.

Particle characterization: DSC analysis

Figure S2 shows the thermographs of the pure substances, for reference. The two polymorphs of menthol racemic mixture melts at 28°C and 38°C respectively: only a very minor fraction of the first one is present in the material as received, while the main melting peak of menthol is observed at 38°C. If the sample is previously premelted at 40°C and cooled, different melting peaks appear, correspondent to different polymorphs.

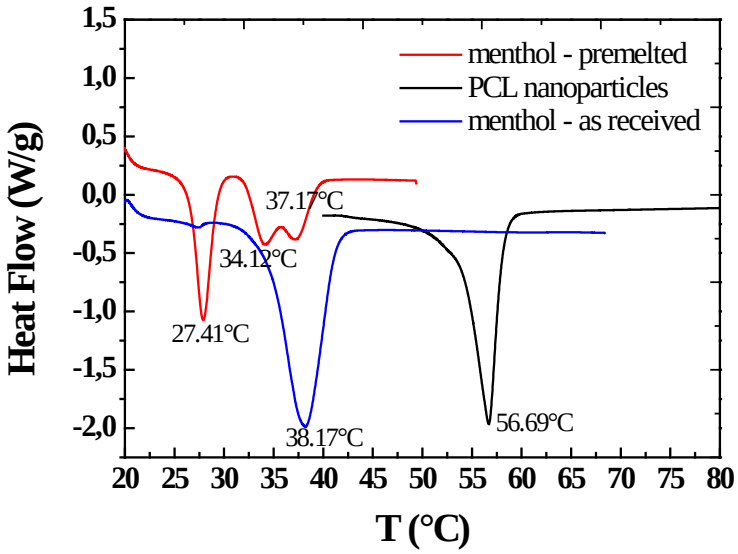

Figure S2. DSC thermograph of menthol and PCL nanoparticles (C_{PCL} = 25 mg/mL); menthol was analysed as received and after melting and solidification. Heating rate: 5°C/min

PCL dissolved in acetone and precipitated in the CIJM (without any menthol) shows a melting temperature around 56°C (experimental data in different samples range from 55.7 to 56.7°C); rapid precipitation from the solvent freezes the PCL structure in a partially amorphous arrangement, as confirmed by the evaluation of the melting enthalpy [theoric PCL melting enthalpy is 134.9 kJ/kg (C. G. Pitt, *Drugs Farm. Sci*. **1990**, 45, 71)].
Figure S3(a) shows a cyclic thermograph of another sample of PCL nanoparticles; in this case the sample is first heated up to 100°C and melted, cooled to 20°C (it can be seen that crystallisation takes place) and then heated up again, always at 5°C/min. It can be noted that the PCL main melting peaks is slightly shifted at lower temperature in the second cycle, which confirms that the melting temperature is affected by the degree of crystallinity and thus by the formation conditions.
A thermograph of loaded nanoparticles is shown in Figure S3(b); it appears very similar to that of pure PCL, as it does not show any menthol melting peak, but only a single melting peak practically at the same temperature of pure precipitated PCL. Samples of NPs prepared in different conditions showed very similar thermographs. This confirms that the encapsulated menthol is either dispersed in the amorphous fraction of PCL, or it forms an amorphous core in the nanoparticles
Some tests have been carried out holding the sample at 40°C, before cooling it to 25°C and heating at 5°C/min (see R. Mossotti et al., *J. Microencapsul.* **2015**, *32* (7), 650). These DSCs resulted different from the previous ones, as melting peaks at different temperature appeared; they are difficult to be interpreted, because the peak temperatures vary depending on the inlet polymer and menthol concentrations, but confirm the encapsulation of menthol.

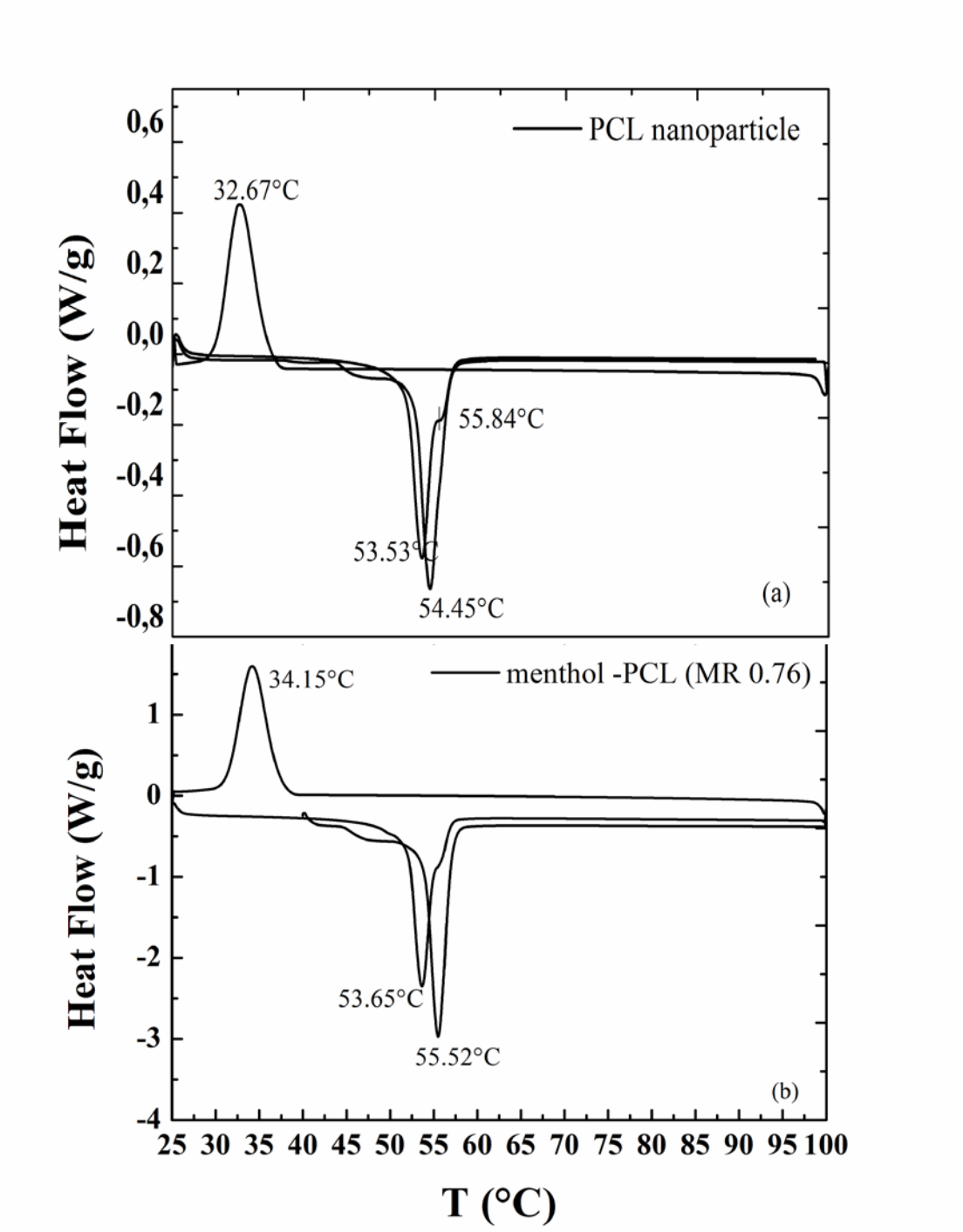

Figure S3. DSC thermograph: (a) PCL nanoparticles, C_{PCL} = 25 mg/mL; (b) menthol-loaded nanoparticles, C_{PCL} = 6 mg/mL, *MR*=0.76. Cyclic heating from 20°C to 100°C; heating and cooling rate: 5°C/min

Particle size distribution (PSD), Polydispersity index (PdI) and Zeta potential

The effect of solvent on menthol-loaded nanoparticle size was similar to that observed for unloaded PCL nanoparticles, namely the smallest particles were obtained with acetone, and larger with acetonitrile. Also the PdI varies in the same way for the different solvents. Some examples of the reconstitued PSD obtained with different quench ratios *QR* are shown in Figure S4 .

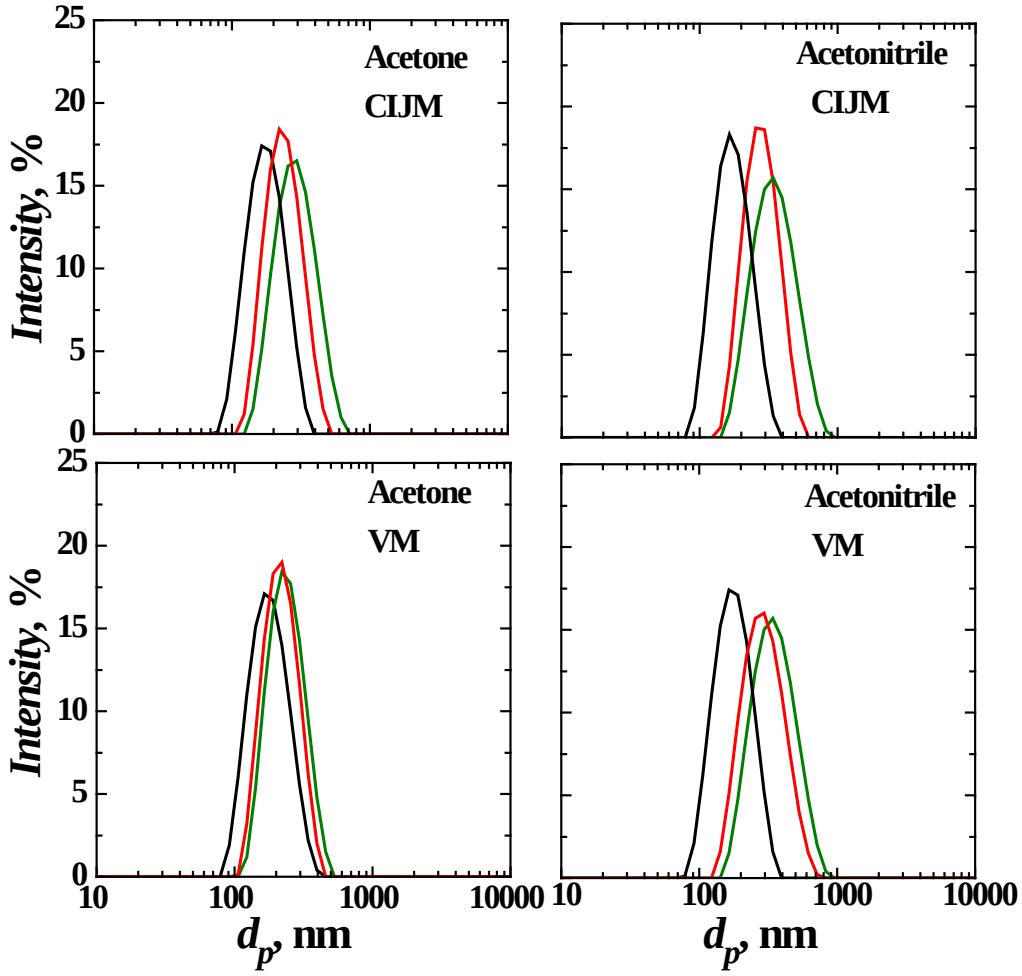

Figure S4. Particle size distribution (PSD) of menthol-loaded nanoparticles using acetone (left graphs) and acetonitrile (right graphs), in CIJM (upper graphs) and two-inlet VM (lower graphs). Quench ratio, *QR*: 0.12 black solid lines; 0.5 red solid lines; 1.0 green solid line. Inlet feed, C_{PCL}= 6 mg/mL, *MR*=0.76. Inlet feed velocity *Vj*=1.69 m/s (*FR*= 80 mL/ min).

An example of the particle size distribution obtained for loaded nanoparticles at different polymer concentration (and constant *MR*) is shown in Figure S5; it can be noted that increasing the PCL concentration the average sinze increases sligthly, but the dsitribution becomes broader.

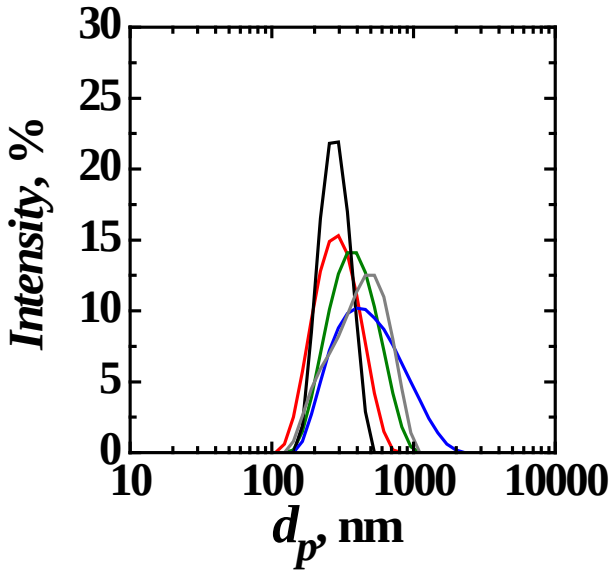

Figure S5. PSD of menthol-loaded nanoparticles produced in the CIJ mixer at different inlet stream velocity using acetonitrile, at menthol/PCL *MR*=0.76 and polymer concentration: $C_{PCL=}$ 3 mg/mL, black lines; 6 mg/mL, red lines; 9 mg/mL, green lines; 12 mg/mL, grey lines; 15 mg/mL, blue lines. Inlet feed velocity *Vj* =0.21 m/s. CIJM, *QR*=0.5.

This is confirmed by the analysis of the polydispersity index (see Figure S6) which shows that polydispersity is also significantly affected by the menthol/PCL ratio.

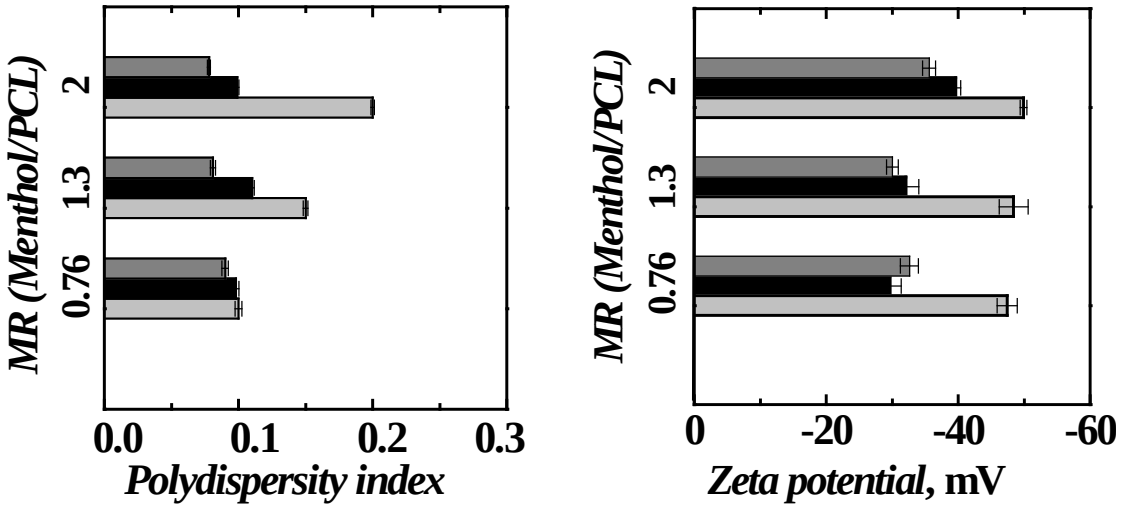

Figure S6. Polydispersity index (left) and Zeta potential (right) of menthol-PCL loaded nanoparticles in acetonitrile; a) *MR*=0.76; b) *MR*=1.3; c) *MR*=2.0. CIJM, *QR*=0.5. Inlet polymer concentration, C_{PCL}: 3 mg/mL, dark grey bars; 6 mg/mL, black bars; 9 mg/mL, light grey bars.
Inlet feed velocity *Vj* =0.21 m/s.

The effect of the different feeding configurations for the vortex type mixers is shown in Figure S7, that also shows the comparison for the two- and four-inlets vortex mixers, both for unloaded nanospheres and for menthol-loaded nanoparticles. The influence of the solvent in this mixer is the same previously reported for the CIJM, with systematically larger particles formed in acetonitrile.

The smallest particles were obtained in the SWWW (that is one solvent and three water streams) configuration; small differences are noted in the symmetrical and non-symmetrical configuration, with the water and solvent streams alternated (SWSW) or in sequence (SSWW) respectively.

As concerns the Zeta potential, the differences between the different configurations were small and, also for the vortex type mixers, values observed for loaded and unloaded particles were similar.

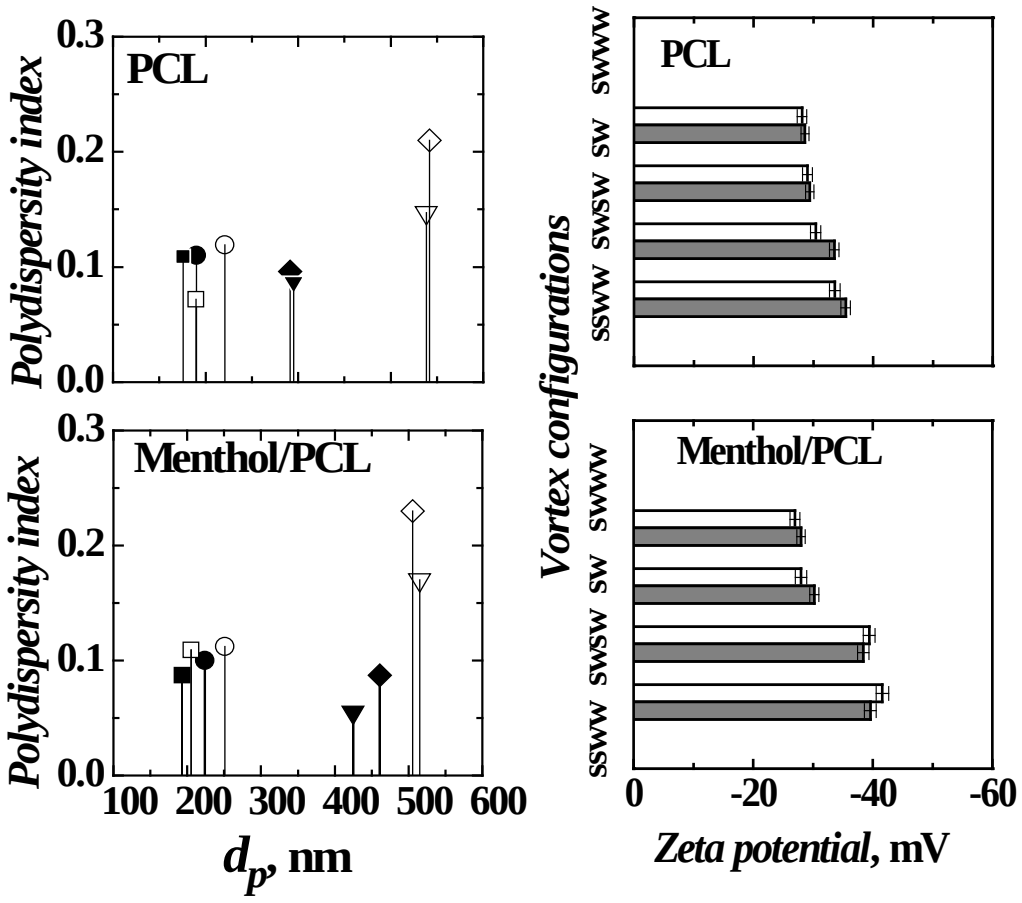

Figure A7. Polydispersity index (left graphs) and Zeta potential (right graphs) of the nanoparticles produced with acetone and acetonitrile, for unloaded polymer nanospheres [PCL] and menthol-loaded nanoparticles [Menthol/PCL]. Left graphs: (a,b) Two-streams VM: ●,○. (*QR*=1). Four streams MIVM: ■,□, SWWW (no quench); ◆◇, SWSW (*QR*=1); ▼,▽, SSWW (*QR*=1). C_{PCL} =6 mg/mL, *MR*=0.76. Inlet feed velocity *Vj*=1.69 m/s. Right graph: (c,d) grey bars for acetone, white bars for acetonitrile. [Note that for the VM the data refer to a different experiment with respect to that shown in Figure 5h]